Bistatic Radar Cross-Sections of Low-Signature Targets

Hans C. Strifors
Swedish Defence Research Agency (FOI)
Department of Sensor Technology
P. O. Box 1165
SE-58111 Linköping
Sweden

hans.strifors@foi.se

ABSTRACT

The main concern when objects are designed for low observability in radar frequency bands is monostatic radar cross-section (RCS) in selected threat sectors. If bistatic scattering is at all considered, only small or moderately large bistatic angles are in general considered. In such cases, it can be tacitly assumed that the magnitude of the bistatic RCSs is comparable to the monostatic RCS in each selected aspect. This assumption could however be unwarrantable for large bistatic angles, which is demonstrated for a target of simple shape. The discussion is based on exact mathematical form of radar cross-sections of a metal sphere, bare or equipped with an efficient microwave absorbing coating. While bistatic RCS in the back-scattering half space is efficiently reduced by the absorbent, the magnitude of the RCS in a forward-scattering sector is very large whether an absorbent is applied to the target or not. If the obtained results should prove adequately general, it means that bistatic, or multistatic, radars could be made to detect low observable (LO) targets of the real world.

1.0 INTRODUCTION

Traditionally, the objective of low observable (LO) technology is to design prospective targets so as to present only a minute radar cross section (RCS) in each threat sector, when they are illuminated in (broad) frequency bands in a monostatic mode (transmitter and receiver at the same location). It is a recognized fact that objects cannot be designed to present diminutive scatter in every direction, which, in turn, would in fact imply the possibility to counter LO targets (air, land, or sea based) using bistatic radar systems (transmitter and receiver at different locations). This issue is here addressed through the investigation of the bistatic scattering in all directions for a radar illuminated object of simple shape. Being sufficiently general for the present purpose, a perfectly conducting sphere is chosen as target, either bare or coated with a thin, lossy dielectric layer.

An obvious advantage of the selected geometry is that exact mathematical analysis applies [1], [2]. The exact solution for scattering from a (perfectly conducting) sphere is traditionally attributed to Mie [3]. The solution employs vector wave functions defined in a spherical coordinate system. Boundary conditions are then used to determine the terms of the resultant series for the scattered field. Over the years, that solution has been generalized in various ways. Aden and Kerker [4] solved the scattering problem for two concentric spheres, which applies to a metal sphere with a homogeneous dielectric layer, thin or thick.

A distinguishing property of dielectric coatings used for reducing the RCS of objects is that the index of refraction is a *complex-valued* function of the frequency due to a complex dielectric permittivity or magnetic permeability, or both. The presence of complex arguments, often with a large imaginary part, in the scattering coefficients severely restricts successful numerical evaluation using traditional algorithms for

Paper presented at the RTO SCI Symposium on "Sensors and Sensor Denial by Camouflage, Concealment and Deception", held in Brussels, Belgium, 19-20 April 2004, and published in RTO-MP-SCI-145.

the Bessel and Hankel functions that appear in the series solutions. Ordinary recurrence relations become unstable. However, modifying an algorithm developed by Lentz [5] renders the numerical evaluation of the scattering coefficients unconditionally stable [2] and numerical evaluation reliable.

2.0 STEADY-STATE SCATTERING AND RADAR CROSS-SECTIONS

Using the series solution in the far field limit and the evaluation algorithms developed in Ref. [2] the scattering at selected frequencies is computed when the target is illuminated by a continuous, plane electromagnetic wave that is horizontally polarized. The target is a metal sphere of diameter 50 cm, and it is either bare or coated with a thin dielectric layer. For the hypothetical layer material the dielectric permittivity and magnetic permeability are assumed to be complex-valued constants (namely, $\varepsilon_r = 20 - 10i$ and $\mu_r = 18 - 9i$), and the layer thickness is chosen to be 0.5 cm. (This layer design corresponds to coating "B" in Ref. [2].) The performance of this microwave absorbent can be readily estimated when it is applied to a plane metal plate and the power reflection coefficient of the coated plate is calculated in the frequency band of 0–10 GHz. The result is displayed in Fig. 1.

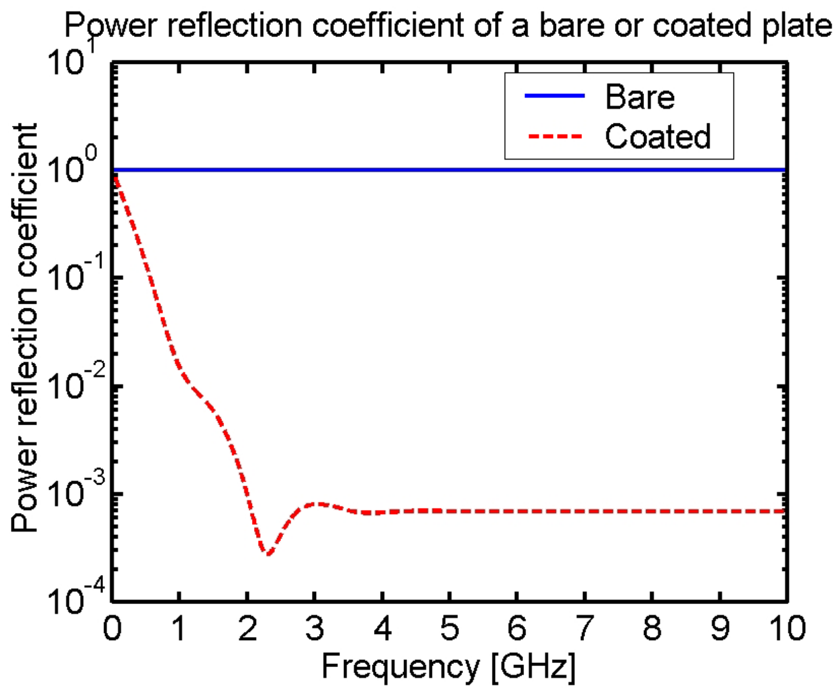

Figure 1: Power reflection coefficient of a metal plate, bare or covered with the designed microwave absorbent.

It is moreover instructive to compare the power reflection coefficient with the modulus of the normalized, monostatic RCS for the bare or coated metal sphere in the same frequency band. The modulus, or magnitude, of the monostatic RCS of the two targets are displayed in Fig. 2, where the blue, solid line shows the RCS of the bare metal sphere and the red, dashed line the RCS of the coated sphere. At lower frequencies, the RCS exhibits the peaks and dips characteristic of the influence of the secondary surface-wave returns. In particular, the power reflection coefficient of the coated plate is practically identical to the normalized RCS for the coated sphere at frequencies larger than about 1 GHz, where the influence of the creeping-wave returns has dropped off.

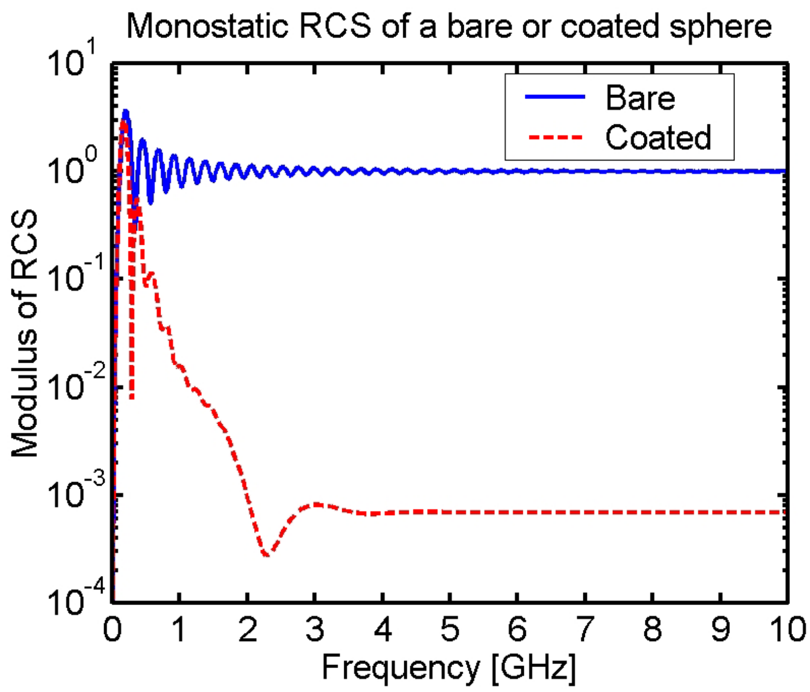

Figure 2: Modulus of the normalized RCS of a metal sphere of diameter 50 cm, bare or covered with the designed microwave absorbent.

3.0 BISTATIC RADAR CROSS-SECTIONS OF TARGETS

For each target (that is, the bare or coated metal sphere), bistatic RCS will now be considered at a few selected frequencies. The target can be thought of as being located at the origin of the coordinate system in the figures below when it is illuminated by a horizontally polarized, continuous wave traveling from left to right. The RCS of the horizontally polarized and the vertically polarized scattered waves are added together to give the target's total RCS, a measure of the *entire scattered energy*. The bistatic total RCS is generated with a direction resolution of one degree in both azimuthal and latitudinal directions. The magnitude of the RCS is then presented as a three-dimensional surface in a logarithmic scale. The distance of the surface from the origin in any given direction is proportional to the logarithm of the magnitude of the RCS in that direction. To enhance the perception of size, the three-dimensional surface is also colored using an arbitrary color scale (pseudocolors).

For the graphic representation, each value of the RCS is first multiplied by ten before the logarithm to the base ten is calculated. If negative, the logarithmic value is then set equal to zero. This means that magnitudes of the normalized RCS less than 0.1 are represented by the distance zero from the origin in the figures and the value *one* by the distance *one*. By this method, it is avoided that small RCS values with negative logarithms that occur in various directions for the coated metal sphere appear in figures as "spears" protruding in the opposite direction. This, in turn, renders the figures below more easily comprehensible.

Figure 3 displays the total normalized RCS of the scattered energy of the bare metal target when the frequency of the incident wave is 1 GHz. At this frequency, the normalized backscattering RCS (BRCS) is about 0.8 (in agreement with Fig. 2) and the forward-scattering RCS (FRCS) about 31. It is clear from Fig. 3 that the total RCS is substantial in most directions for this simple-shaped target.

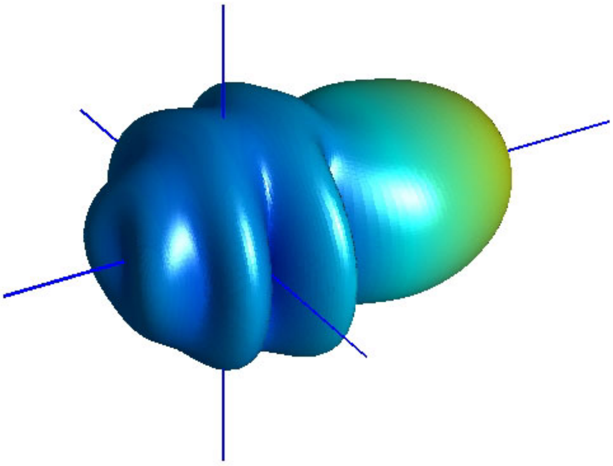

Figure 3: Total normalized RCS of the bare metal sphere at the frequency 1 GHz.

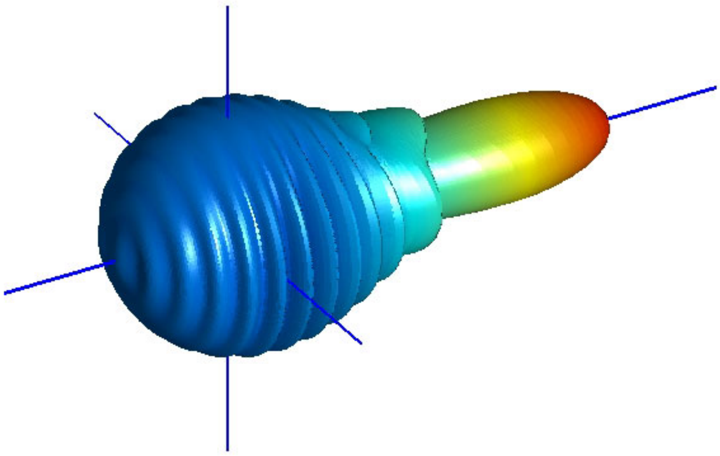

Figure 4: Total normalized RCS of the bare metal sphere at the frequency 3 GHz.

The corresponding total RCS when the incident wave has frequency 3 GHz is displayed in Fig. 4. In the backscattering half space (that is, for bistatic angles less than 90º) and in a large sector of the forward-scattering half space the magnitude of the RCS is close to *one*, the approximate value of the BRCS. For still larger bistatic angles the magnitude increases to reach the value of about 250 for the FRCS, which is much larger than for the lower frequency of 1 GHz. Figures 5 and 6 convey the idea of the general trend of the RCS when the frequency of the incident wave increases even more. While the normalized RCS in most directions is close to *one*, the FRCS is about 670 at 5 GHz and 2300 at 10 GHz.

In optics, the highly peaked forward-scattering lobe is in fact quite well-known [6]. For instance, driving a car toward a bright setting sun can be an extremely glaring experience, even if the direct sunbeams are blocked by the car's roof or sun visor. The reason is the forward-scattering from particles in the air or on the windshield, or both. There also exist halo phenomena with a similar physical basis.

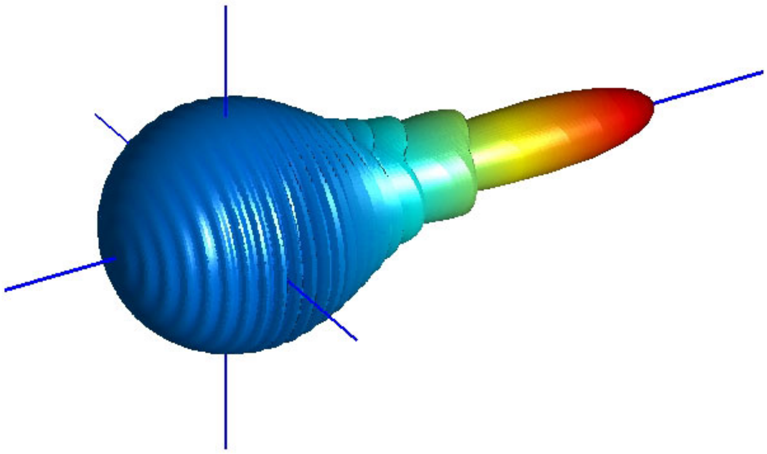

Figure 5: Total normalized RCS of the bare metal sphere at the frequency 5 GHz.

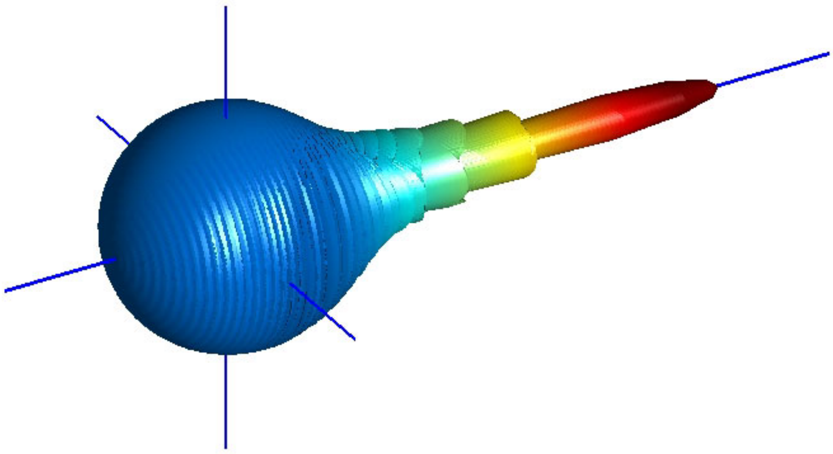

Figure 6: Total normalized RCS of the bare metal sphere at the frequency 10 GHz.

The focus will now be shifted toward the scattering interaction of waves with the metal sphere when it is equipped with the absorbent layer specified above. The total normalized RCS of that target when it is illuminated by a horizontally polarized wave of frequency 1 GHz is displayed in Fig. 7. It can be seen that in the backscattering half space the absorbent is quite efficient. The normalized BRCS is, in fact, less than 0.02, which can be read off from Fig. 2, red dashed line. However, in most of the forward-scattering half space scattered waves of significant magnitude indeed occur, and the magnitude of the total FRCS is about 56. This value is almost twice as large as the FRCS for the bare sphere. On the other hand, the sector of very large RCS values is somewhat narrower. This can be compared with the target's RCS when the incident wave has the frequency 3 GHz, which is shown in Fig. 8. The BRCS is now of the order of 10^{-3} and the magnitude of the FRCS about 360.

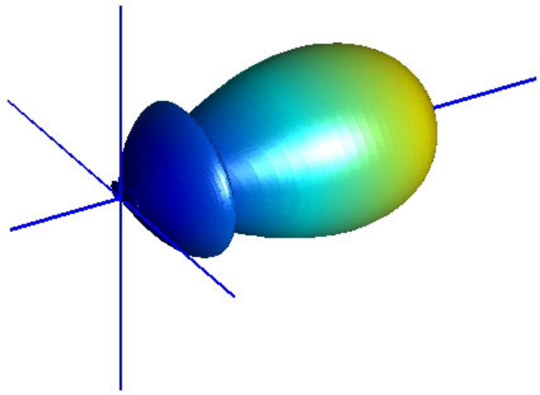

Figure 7: Total normalized RCS of the coated metal sphere at the frequency 1 GHz.

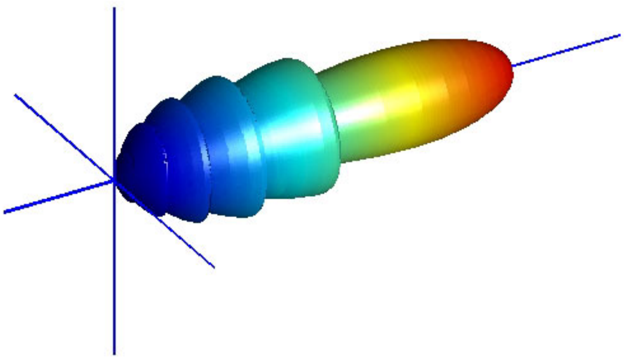

Figure 8: Total normalized RCS of the coated metal sphere at the frequency 3 GHz.

The total RCS for the coated sphere when the frequency of the illuminating wave is 5, or 10, GHz is displayed in Fig. 9, or 10. As can be expected, the BRCS is also in these cases of the order of 10^{-3}. The magnitude of the FRCS is about 880 and 2700, respectively. For each frequency, the magnitude of the FRCS is also in these cases larger for the coated sphere than for the bare one, while the forward-scattering sector of giant RCS values is slightly narrower. This trend has been observed also for other targets and absorbents.

Even though the forward-scattered energy cannot be used for detection purposes, there indeed exists a useful forward-scattering sector where the RCS is large enough whether the target is coated or not. For instance, when the bistatic angle is 120º, the RCS for the coated sphere is larger than about one tenth of the monostatic RCS for a bare sphere, and the RCS then increases with increasing angle.

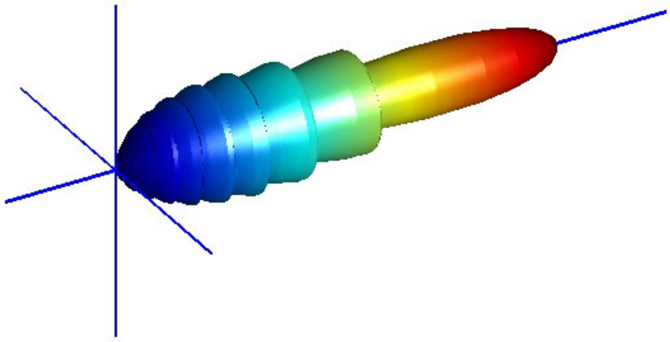

Figure 9: Total normalized RCS of the coated metal sphere at the frequency 5 GHz.

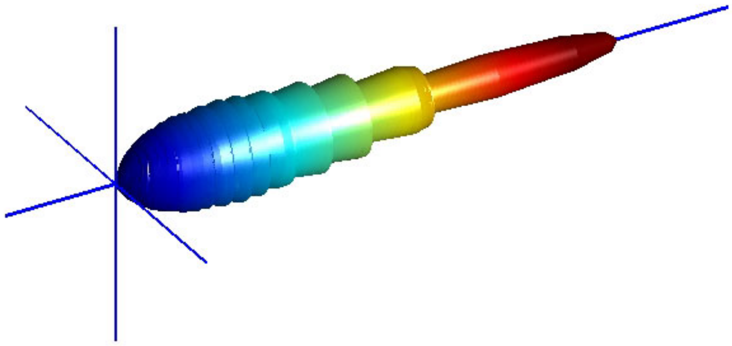

Figure 10: Total normalized RCS of the coated metal sphere at the frequency 10 GHz.

4.0 INTERPRETATION AND INFERENCES

The scattering interaction of a target with incident waves of a few different frequencies was investigated. The target was a metal sphere of diameter 50 cm, either bare or equipped with a thin, efficient radar absorbing coating. The scattered electromagnetic energy and the corresponding radar cross-section (RCS) were computed in all (bistatic) directions. The backscattering and forward-scattering characteristics can be conveniently studied from the obtained results, and the effectiveness of the microwave absorbent appreciated. In particular, it was demonstrated for the coated target that, while the reduction of the RCS may be quite substantial in the backscattering half space (that is, for bistatic angles less than 90º), the RCS reduction dwindles as the bistatic angle increases above 90º. The magnitude of the RCS is very large in a narrow sector close to the forward-scattering direction, whether the target is coated with a microwave absorbing layer or not.

A forward-scattered wave cannot be used for radar detection, because the wave incident on the target propagates in the same direction and is a lot stronger. However, apart from a narrow sector around the forward-scattering direction, the bistatic RCS could nonetheless be significant enough for detection in a sector of practicable width (bistatic angles larger than 120º, say). Furthermore, very low frequencies, or very large wavelengths (compared with characteristic dimensions of the target), drastically widens the useful sector of large bistatic RCS.

Do the presented results qualify any far-reaching inference? Few targets of interest to the radar community have spherical shape. On the other hand, the shape of a target becomes less significant when the radar operates in a very low frequency band. This fact leads up to the surmise that any target, when it is illuminated by a wave of sufficiently low frequency, would generate bistatic RCS in the forward-scattering half space that bear a resemblance to Fig. 3 or 7, depending on whether or not LO technology has been used in the target's design. Moreover, it is evident from the obtained results that a radar absorbing material possibly will be incapable of reducing the RCS in a forward-scattering sector for *any* target, however effective it may be in the backscattering half space.

Finally, exact scattering solutions for targets with highly absorptive materials in their composition can be formulated only for targets of simple geometric shape. Geometric shaping as a means in LO design is not considered here. Nevertheless, exact scattering solutions are undeniably valuable as benchmark for numerical algorithms and codes. This is particularly true for the reason that the accuracy of numerically calculated radar cross-sections is imperative in LO technology.

5.0 REFERENCES

[1] G. T. Ruck, D. E. Barrick, W. D. Stuart, and C. K. Krichbaum, *Radar Cross Section Handbook*, vol. 1. New York, NY: Plenum, 1970.

[2] H. C. Strifors and G. C. Gaunaurd, "Scattering of Electromagnetic Pulses by Simple-Shaped Targets with Radar Cross Section Modified by a Dielectric Coating," *IEEE Trans. Antennas Propagat.*, vol. 46, pp. 1252–1262, Sept. 1998.

[3] G. Mie, "Beiträge zur Optik trüber Medien, speziell kolloidaler Metallösungen," *Ann. Phys.*, vol. 25, pp. 377–445, Mar. 1908.

[4] A. L. Aden and M. Kerker, "Scattering of electromagnetic waves from two concentric spheres," *J. Appl. Phys.*, vol. 22, pp. 1242–1246, Oct. 1951.

[5] W. J. Lentz, "Continuous fraction calculation of spherical Bessel functions," *Comput. Phys.*, vol. 4, pp. 403-407, Jul./Aug. 1990.

[6] C. F. Bohren and D. R. Huffman, *Absorption and Scattering of Light by small Particles*, New York, NY: John Wiley & Sons, 1983.